Hobson, E. W., "The Theory of Spherical and Ellipsoidal Harmonics," Cambridge Univ. Press, 144–63 (1931).
Neogi, P., and E. Ruckenstein, "Transport Phenomena in Solids with Bidisperse Pores," *AIChE J.*, **26**, 787(1980).
Rocha, A., and A. Acrivos, "On the Effective Thermal Conductivity of Dilute Dispersions: General Theory for Inclusions of Arbitrary Shape," *Quart. J. Mech. Appl. Math.*, **26**, 217(1973).
Ruckenstein, E., "The Effectiveness of Diluted Porous Catalysts," *AIChE J.*, **16**, 151(1970).
Varghese, P., and E. E. Wolf, "Effectiveness and Deactivation of a Diluted Catalyst Pellet," *AIChE J.*, **26**, 55(1980).

Manuscript received March 2, 1981; revision received September 14, and accepted October 13, 1981.

APPENDIX

We solve here the equation

$$\nabla^2 C = \beta C \tag{i}$$

since both Eqs. 27 and 15 are of this form with constant β. C in Eq. i is subject to boundedness and to the condition that

$$C|_{r=r_o} = C_o \tag{ii}$$

where r_o is the radius of the macrosphere. Thus, C is a function of r only and the solution to Eq. i subject to Eq. ii becomes

$$C = C_o \frac{\sinh(r\sqrt{\beta})}{\sinh(r_o\sqrt{\beta})}\left(\frac{r_o}{r}\right) \tag{iii}$$

Then the total flux to the sphere is

$$F(\beta) = -\epsilon_\beta D_\beta 4\pi r_o^2 \left.\frac{\partial C}{\partial r}\right|_{r=r_o} \tag{iv}$$

and the ratio

$$\eta = \frac{\text{flux to the diluted catalyst}}{\text{flux to the undiluted catalyst}}$$

becomes

$$\eta = \alpha \frac{[\theta \coth(\theta) - 1]}{\left[\frac{r_o}{r_i} x \coth\left(\frac{r_o}{r_i} x\right) - 1\right]} \tag{v}$$

with

$$\theta^2 = 3\phi\left(\frac{r_o}{r_i}\right)^2 \frac{1}{2 + \alpha[x \coth(x) - 1]^{-1}}$$

on identifying β, D_β and ϵ_β from Eqs. 27 and 15

Dynamic Studies of Dispersion and Channeling in Fixed Beds

An experimental and theoretical study was carried out to relate the extent of channeling in a packed column to the response in the effluent gas to a tracer input. When the response curve showed a distinct peak associated with a channel, it was possible to establish the flow rate and void area of the channel from only the response curve. The experimental data provided new information on Peclet numbers in packed columns with nonuniform void fractions (low tube-to-particle diameter ratios).

GABRIEL OLIVEROS
and J. M. SMITH
University of California, Davis
Davis, CA 95616

SCOPE

Nonuniform void regions in packed beds may be due to the influence of the column wall or may result when the packing process itself is nonuniform. Such nonuniformities cause channeling of flow with adverse performance: for example, reduced conversion or selectivity in fixed-bed catalytic reactors. While packing nonuniformities are usually random, the response curve to a tracer input provides some evidence of the specific characteristics of flow maldistribution. Thus, two, more-or-less distinct peaks in the response to a pulse input of tracer, or a peak with an elongated tail, are suggestive of channeling. However, the response can also be distorted by axial dispersion for a nonadsorbable tracer and, in addition, by adsorption for a tracer adsorbable on the packing.

For beds where nonuniform void fractions are suspected, it would be helpful to be able to determine quantitatively the extent of channeling from the overall response curve; that is, to determine the flow rate through the channels and their void areas. Our purpose in this paper is to report results of comparing predicted channeling with experimental measurements in beds prepared intentionally with a nonuniform distribution of voids. This was done in a simple way by packing glass beads in the annulus and core regions of a cylindrical column. The void fractions in the annulus and core could be varied by using different sizes of glass beads and by varying the width of the annulus and diameter of the core. To ensure large void fractions, and encourage channeling, low ratios (1.8 to 12) of width-(or diameter)-to-particle diameter were used. A nonadsorbing tracer (helium) was introduced into air (at 298 K and 101 kPa) entering the column, and the response curve measured in the combined effluent.

CONCLUSIONS AND SIGNIFICANCE

The experimental response curves for several bed arrangements showed two, more-or-less distinct peaks. In all cases these arrangements included a thin aluminum screen separating the core and annulus (noninteracting case). For such cases it was possible to estimate the effects of axial dispersion (Peclet numbers) on the response curves so that reliable values of the flow rates and void areas could be calculcated. The information required, in addition to the response curve, is the overall flow

rate, overall void fraction and the overall diameter and length of the column. The effect of axial dispersion could be accounted for by deconvoluting the response curve, or by using an available correlation for the Peclet number for uniform beds when the core-to-particle diameter ratio was relatively large (>10). An approximate prediction method, based upon the time corresponding to the maximum concentration in the response peak for each section, was investigated. This approach, which did not require Peclet numbers, gave more accurate predictions as the response peaks for the core and annular regions became more distinct. Except for cases where the response peaks were not distinct, results predicted by this method were as nearly as accurate as those obtained by the more complex methods requiring Peclet numbers.

The deconvolution method and the measured response curves gave new information about Peclet Numbers in beds with small width (δ_a)-to-particle size ratios. These values of Pe were less than those for large ratios (uniform beds). The results could be reproduced when the ratio was 4 or more, but were specific for the particular packing arrangement for δ_a / d_p of 1.8. It is concluded that a bed cannot be repacked reproducibily for such low ratios.

When but one peak is observed, so that channeling only affects the tail, we were unable to predict the extent of channeling. These kind of responses were observed for one arrangement (column #5) for the noninteracting case and for all conditions for the interacting case (only a screen separating the core and annulus). The radial transport of tracer in our small-diameter apparatus (overall ID = 0.0837 m) was sufficiently rapid to disguise most effects of channeling when there was no barrier between core and annulus. In contrast, our noninteracting data may well correspond to the interacting case for large-diameter beds such as exist in *in-situ* oil-shale retorts.

Pressure drop measurements through the beds did not provide a useful relationship in our experiments. The Δp results did not accurately obey the Ergun equation. Also, the accuracy of the data was limited by the small magnitude of Δp in our relatively short (0.60 m) beds.

In analyzing processes involving fluids flowing through packed beds, it is customary to consider the void fraction to be uniform. For large diameter beds, carefully packed with small particles of the same size, this procedure is satisfactory. However, when there is a non-uniform distribution of particles, void-fraction variations result in channels of fluid flowing at different velocities.

Channeling is a common cause of poor performance in fixed-bed processing; for example, conversion is reduced in catalytic reactors. The problem is particularly important in trickle-bed units where maldistribution of liquid can be severe. A different, large-scale example occurs in *in-situ* retorting of oil shale. Here difficulties in achieving uniform beds can lead to multiple channels. The end result is incomplete retorting of the bypassed parts of the bed.

Radial variation in void fraction in cylindrical beds due to wall influence, is well established (Schwartz and Smith, 1953; Stanek and Eckert, 1979). This type of non-uniformity, and the channeling of flow that results, is reproducible, relatively mild, and can be accounted for with a pseudo-continuous velocity profile. We are concerned with a different type of channeling: the more severe form due to larger more discrete changes in void fraction due to non-uniform packing. The objective is to relate the response of a tracer input to the extent of dispersion and channeling. The ideal result would be to predict quantitatively the void fraction and flow rates in the channels from only the response curve measured in the total effluent from the bed. This is a difficult objective, and requires a knowledge of axial dispersion (Peclet numbers) in the channels. Some success is possible if channeling is sufficiently severe to give more or less distinct peaks in the response curve.

In order to evaluate prediction methods for dispersion and channeling, response curves were measured for cylindrical, packed beds purposely prepared with non-uniform void fractions. This was done by filling annular and core sections of variable diameter with spherical particles of different sizes. The double-wall effect in the annulus was used to obtain a high porosity with respect to the porosity in the core. Data were obtained for both a non-interaction arrangement (thin aluminum foil covering a stainless steel screen separating core and annular regions) and for the interaction case where only the screen (opening = 0.004 m) separated the two sections. For our experimental conditions, particularly the small bed length and section diameters, the interaction data could not be analyzed to establish the extent of channeling, because the response curve contained but one concentration peak and differed but slightly from the response to a uniform bed. Our small-scale experiments of the non-interaction type probably simulated, more closely than the interaction experiments, the behavior of large-diameter beds such as in-situ, oil-shale retorts.

EXPERIMENTAL STUDIES

Figure 1 shows the apparatus used to introduce a pulse of pure helium into air flowing through a packed bed. The 6-port sampling valve used to inject the helium pulse, and the TC detector for analyzing the bed effluent, were closely connected to the bed in order to minimize end effects. Figure 2 depicts the packed column. The packed-bed depth (0.594 m) was large with respect to the unpacked lengths (0.01 m) so that the dead volumes, between injection and entrance to the bed and between bed exit and TC detector, had a negligible effect on the shape of the response curve. This was ascertained from preliminary pulse-response experiments with no bed.

The screen (thickness 0.0018 m) was positioned in the column (ID = 0.0837 m) so that the core ID was either 0.0383 or 0.0582 m. Measurements were made at room temperature and atmospheric pressure for overall superficial velocities from 0.38 to 1.2×10^{-2} m/s.

The packed beds were prepared by first filling the core section with the glass beads. After each addition of 0.05 m height of bed, the column was shaken thoroughly. After the core cylinder was filled it was placed in the column and attached to the support. The core section was then filled slowly and as uniformly as possible. The void fractions in core and annulus were determined from the densities of the glass beads, the weight of each section, and the dimensions of each section. The densities and particle diameters were:

Particle Diameter m	Particle Density kg/m³
0.004	2.6680
0.005	2.5553
0.006	2.5520

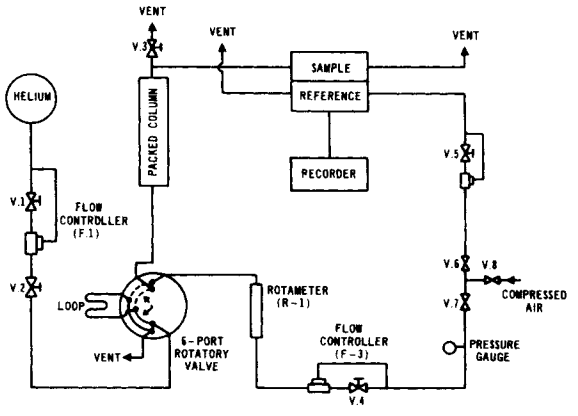

Figure 1. Schematic diagram of the apparatus.

TABLE 1. DIMENSIONS AND VOID FRACTIONS FOR THE FIVE EXPERIMENTAL COLUMNS

Column No.	Core I.D. m	Core Void Fraction ϵ_c	Core Part. Size d_p, m	Annulus Width δ_a, m	Annulus Void Fraction ϵ_a	Annulus Part. Size d_p, m	Overall Col. I.D. m	Overall Void Fraction ϵ	Overall Col. Length L, m
1	0.0582	0.40	0.004	0.0109	0.45	0.006	0.0837	0.42	0.594
2	0.0582	0.40	0.004	0.0109	0.42	0.005	0.0837	0.41	0.594
3	0.0582	0.38	0.005	0.0109	0.45	0.006	0.0837	0.42	0.594
4	0.0383	0.36	0.004	0.0209	0.43	0.006	0.0837	0.41	0.597
5	0.0383	0.35	0.004	0.0209	0.41	0.005	0.0837	0.40	0.597
5R		0.37			0.42			0.41	

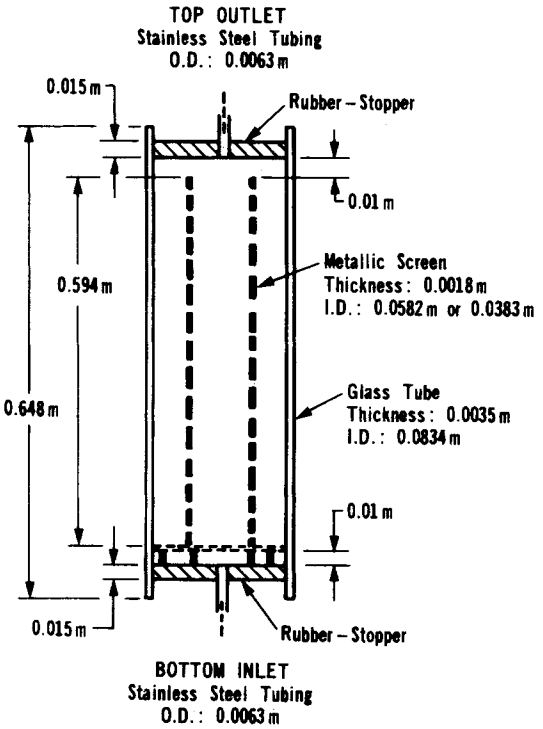

Figure 2. Diagram of the packed column.

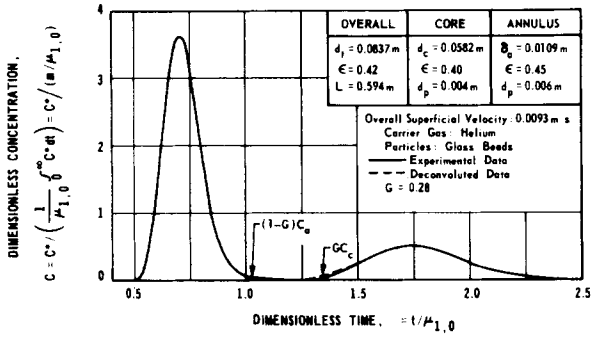

Figure 3. Experimental and deconvoluted response curves: Column No. 1, Run #4, noninteraction.

After the column was prepared the apparatus was run overnight at the highest flow rate in order to attain stable operating conditions for the detector. Then response curves were measured for six, successively lower flow rates. One to two hours was required to obtain stable conditions (a very stable base line on the strip-chart recorder) when the flow rate was changed.

Response Curves

Experiments were carried out over a range of gas velocities for five different combinations, of particle sizes and core and annulus radii, described as columns 1–5. These different combinations resulted in different void fractions in the two sections as shown in Table 1. Response curves for the five columns for intermediate velocities are shown in Figures 3–7. For example, the solid curve in Figure 5 for column 3 is for a annular space,

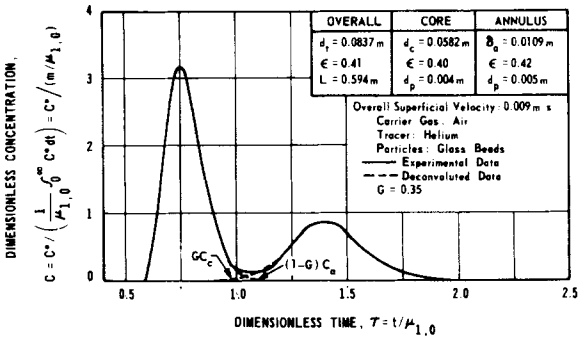

Figure 4. Experimental and deconvoluted response curves: Column No. 2, Run #7, noninteraction.

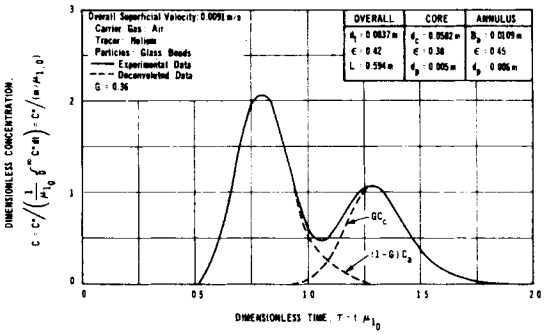

Figure 5. Experimental and deconvoluted response curves: Column No. 3, Run #3, Non-Interaction.

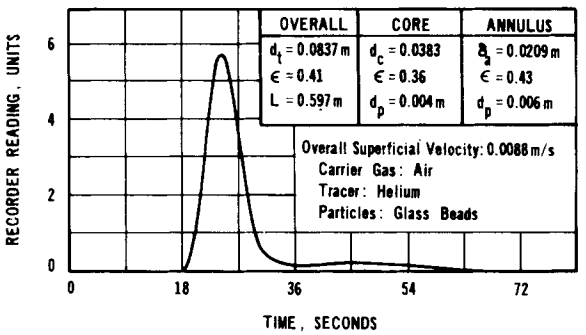

Figure 6. Experimental response curve: Column No. 4, Run #6, noninteraction.

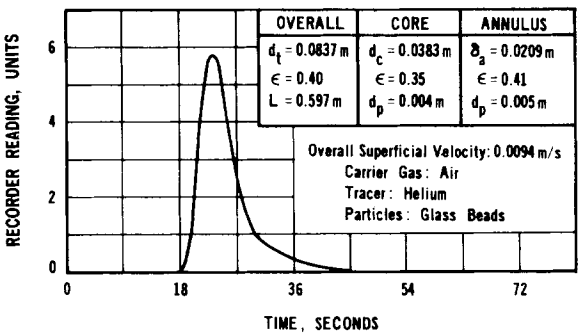

Figure 7. Experimental response curve: Column No. 5, Run #6, noninteraction.

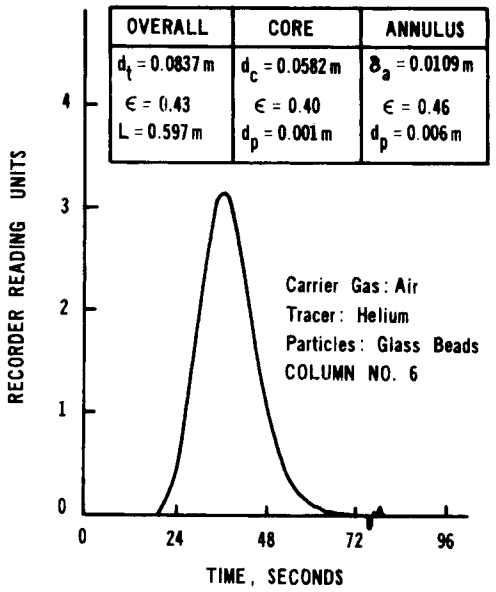

Figure 8. Experimental response curve: interacting regions, Run #4.

δ_a, of 0.0109 m packed with 0.006 m particles. The ratio δ_a/d_p is but 1.8 so that a large void fraction, $\epsilon_a = 0.45$, results. The ratio of core diameter to particle diameter was nearly 12 (5.82/0.5) giving a much lower void fraction $\epsilon = 0.38$. For this combination two distinct peaks were observed in the response curve. In fact for columns 1–3 the ratio of core diameter to particle size was greater than 10, while in the annulus the ratio was about 2. These arrangements lead to severe channeling and all three response curves (Figures 3–5) exhibited distinct peaks. For columns 4 and 5 the ratio in the core was 9 and in the annulus about 4. Channeling was mild and the response curves did not exhibit two distinct peaks but only elongated tails, particularly for column 5 (Figure 7). For the conditions of column 5 measurements were made on a repacked bed (run 5R in Table 1) to test the reproducibility of the results (Figure 13).

For comparison, Figure 8 shows the response curves for the interacting case (no aluminum sheet separating the core and annular regions) for the same particle sizes and core and annulus dimensions as for column 3. Here there is but one peak with a slightly asymmetric shape (elongated tail).

EQUATIONS FOR THE RESPONSE CURVE

An analytical solution is obtained for the response to a pulse input of tracer for the following conditions:

1. No mass transfer between core and annulus (noninteracting case).
2. Isothermal operation.
3. An axial dispersion model superimposed on plug flow, as recommended by Wen and Fan (1975).
4. The Wilhelm and Danckwerts boundary conditions (Danckwerts, 1956; Wehner and Wilhelm, 1956) are valid.
5. The input is a pulse (delta) function.

With these conditions the dimensionless mass conservation equations, for nonadsorbable tracer, and boundary and initial conditions, are:

Mass conservation equations:

$$\frac{1}{b_c}\frac{\partial C_c}{\partial \tau} + \frac{\partial C_c}{\partial Z} = a_c \frac{\partial^2 C_c}{\partial Z^2} \qquad \text{for the core} \tag{1}$$

$$\frac{1}{b_a}\frac{\partial C_a}{\partial \tau} + \frac{\partial C_a}{\partial Z} = a_a \frac{\partial^2 C_a}{\partial Z^2} \qquad \text{for the annulus} \tag{2}$$

Boundary conditions:

$$\left.\begin{aligned} \delta(\tau) &= C_c - a_c \frac{\partial C_c}{\partial Z} \\ \delta(\tau) &= C_a - a_a \frac{\partial C_a}{\partial Z} \end{aligned}\right\} \quad \text{at } Z = 0 \quad \text{for } \tau > 0 \tag{3, 4}$$

$$\left.\begin{aligned} \frac{\partial C_c}{\partial Z} &= 0 \\ \frac{\partial C_a}{\partial Z} &= 0 \end{aligned}\right\} \quad \text{at } Z = 1 \quad \text{for } \tau > 0 \tag{5, 6}$$

Initial conditions:

$$\left.\begin{aligned} C_c &= 0 \\ C_a &= 0 \end{aligned}\right\} \text{at } \tau = 0 \quad \text{for } Z > 0 \tag{7}$$

The dimensionless time is defined with respect to the first moment of the overall response curve, or to the overall void fraction ϵ and overall superficial velocity V_{z3} according to the equations:

$$\tau = \frac{t}{\mu_{1,0}} = \frac{t}{\epsilon L/V_z} = \frac{t}{\epsilon LA/Q} \tag{8}$$

The dimensionless concentration, C, and bed depth, Z, are defined in the Notation as are the parameters a_c and a_a, related to the axial dispersion coefficients, D_{zc} and D_{za}, and b_c and b_a, which are relative interstitial velocities in the core and annulus, respectively. The parameters a_c and a_a are reciprocals of the Peclet numbers based upon the bed length, as shown in Eqs. 21 and 22.

The average concentration in the total effluent from the bed is given by a mass balance of tracer:

$$C(Z,\tau) = C(1,\tau) = G\,C_c(1,\tau) + (1 - G)\,C_a(1,\tau) \tag{9}$$

where G is the fraction of the total volumetric flow rate, $V_{z,c}A_c/V_zA$, going through the core region. Equations 1–8 can be solved (Oliveros, 1981) for $C_c(1,\tau)$ to give

$$C_c(1,\tau,a_c b_c) = \frac{2b_c}{a_c^{1/2}} \exp\left(-\frac{(1 - b_c\tau)^2}{4a_c b_c \tau}\right) \times \left[\frac{1}{(\pi b_c \tau)^{1/2}} + \frac{1}{2a_c}\left(\frac{b_c\tau}{\pi}\right)^{1/2} - \frac{1}{a_c^{1/2}} \times \left(1 + \frac{1}{4a_c} + \frac{b_c\tau}{4a_c}\right) \exp\left(\frac{(1 + b_c\tau)^2}{4a_c b_c \tau}\right) \operatorname{erfc}\left(\frac{1 + b_c\tau}{(4a_c b_c \tau)^{1/2}}\right)\right] \tag{10}$$

The result for $C_a(1,\tau,a_a,b_a)$ is the same as Eq. 10 with the subscript a replacing c. These results can be substituted in Eq. 9 to give an analytical expression for the response curve $C(1,\tau)$ as a function of the four parameters a_c, a_a,b_c,b_a.

The first moments of the combined effluent and the core and annulus sections are equal to the corresponding residence times:

$$(\mu_1)_o = \frac{\epsilon L}{V_z} \tag{11}$$

$$(\mu_1)_c = \frac{\epsilon_c L}{V_{zc}} \tag{12}$$

$$(\mu_1)_a = \frac{\epsilon_a L}{V_{z,a}} \tag{13}$$

From these three equations, b_c and b_a can be expressed as ratios of the first moments:

$$b_c = \frac{\epsilon/V_z}{\epsilon_c/V_{z,c}} = \frac{(\mu_1)_o}{(\mu_1)_c} \tag{14}$$

and

$$b_a = \frac{\epsilon/V_z}{\epsilon_a/V_{z,a}} = \frac{(\mu_1)_o}{(\mu_1)_a} \tag{15}$$

A total mass balance and total void-volume balance provide two more relations between areas, A_c,A_a, void fractions ϵ_c,ϵ_a, and superficial velocities $V_{z,c}$,$V_{z,a}$:

$$V_zA = V_{z,c}A_c + V_{z,a}A_a \tag{16}$$

$$\epsilon A = \epsilon_c A_c + \epsilon_a A_a \tag{17}$$

In principle, the pressure drop across the bed offers an additional relationship between the velocities, void fractions, and particle

diameters. For example, the Ergun equation (Ergun, 1952) may be assumed applicable for the core section. Then if the pressure is measured, the number of parameters necessary to calculate $C(Z,\tau)$ from Eq. 9 is reduced from four to two, a_a,a_c. We attempted to use this procedure and measured the pressure drop with a micromanometer sensitive to 5.6×10^{-6} m of n-butyl alcohol (manometer fluid). However, calculations of the velocity in the core section did not agree with the velocity obtained from the first moment using Eq. 12. The latter evaluation is based upon the measured response curve, as explained later, and gives reliable results. It is concluded that the Ergun equation did not represent the effects of velocity, void fraction and particle size accurately enough for our beds. It may be that part of the problem is due to the small values ($\sim 4 \times 10^{-4}$ m of n-butyl alcohol) and uncertain accuracy of Δp. Details of the application of the Ergun equation are given by Oliveros (1981).

PROBLEM STATEMENT

The prior discussion indicates that to predict the extent of channeling it is necessary to determine the void areas of the annulus and core sections and the fraction of the total volumetric rate in each section. Available is the measured overall response curve and the cross-sectional area and void fraction of the bed as a whole. Equation 9, with Eq. 10 for the core, and a similar expression for the annulus, gives the response curve in terms of the four parameters a_c,a_a and b_c and b_a. Equations 14 to 17 provide the necessary relations to evaluate the section void areas, and section velocities (as flow rates), from b_c and b_a. Optimal fitting of experimental response curves with Eq. 9 is not an accurate procedure for evaluating four parameters. Methods are proposed in the next two sections for reducing the number of unknown parameters. In the first method, applicable when separable peaks occur in the measured response, the measured overall response curve is separated into individual responses for the core and annulus sections. Then the separate curves are used to determine the axial dispersion coefficients D_c and D_a (or Peclet numbers). Data for the different bed arrangements, columns 1–3, provide correlations of the Peclet numbers for each section. These correlations eliminate a_c and a_a. The problem of predicting the extent of channeling is reduced to fitting the measured response curve with a two-parameter (b_c and b_a) equation. The second method uses an existing correlation for the Peclet number for the core section and thus avoids the assumption required for separating the overall response curve into separate curves for core and annulus. Otherwise, the two methods are the same. This second method can be applied where the overall response does not exhibit distinct peaks.

When the overall response curve exhibits two distinct peaks, an approximate third method based upon the times, t_{max}, of the peaks can be used to estimate channeling. This approach avoids parameter evaluation. A comparison of the two methods is given later.

PECLET NUMBERS BY DECONVOLUTION OF OVERALL RESPONSE CURVE

The experimental data provide an overall response curve, and the void fractions and cross-sectional areas for the core and annulus. From this information the Peclet numbers for each section can be evaluated, provided that the measured response curve can be deconvoluted into individual response curves for each section. Data are available for five different columns and for several flow rates for each column. The plan is to use these data to obtain a correlation of the Peclet number as a function of (Re)(Sc).

It was found that the leading branch of the response curve can be accurately represented by a normal distribution. For example, in Figure 3 this means that the left side of the first peak, corresponding to the annulus since it has the higher porosity, represents the leading half of a normal distribution curve. Similarly, the leading half of a deconvoluted response for the second peak, for the core, can be similarly represented. The normal distribution curve is a function of only the time, t_m, corresponding to the maximum concentration and the variance:

$$C_{exp} = C_{exp,m} \exp\left[-\frac{(t-t_m)^2}{2\sigma^2}\right] \tag{18}$$

$$\sigma = \frac{t_m - t}{\left(2 \ln \frac{C_{e,m}}{C_e}\right)^{1/2}} \tag{19}$$

The variances and t_m values for the separate responses for the core and annulus can be evaluated from the leading half of the overall response for the annulus and the trailing half for the core. Using these values separate response curves are obtained for each section. Illustrative results are shown by the dotted curves in Figure 3. The method is described in detail by Oliveros (1981). Inherent in this method is the assumption that the tail of the curve for the annulus does not influence the maximum of the peak for the core. This assumption is seen to be barely satisfied in Figure 3. It is a good assumption for columns 1 and 2 as well, but not for columns 4 and 5. The second method, described in the next solution does not have this restriction.

Once deconvolution has been accomplished, b_c and b_a are readily evaluated from the first moments of the separate response curves by employing Eqs. 14 and 15. Then the separate response for the core can be used with Eq. 10 to obtain an optimal value of a_c. This optimum is determined by minimizing the square of the deviations, F, between the concentrations read from the curve and calculated by Eq. 10:

$$F(a_c) = \sum (C_{c,d} - C_c)_i^2 \tag{20}$$

where $C_{c,d}$ represents the dimensionless concentrations read from the deconvoluted curve and C_c is calculated from Eq. 10. Exactly the same procedure can be used to evaluate a_a for the annular region.

Finally, the Peclet numbers for core and annulus are calculated from the equations

$$Pe_c = \frac{V_{zc} d_{p,c}}{D_c} = \frac{d_{p,c}}{L} \frac{1}{a_c} \tag{21}$$

$$Pe_a = \frac{V_{z,a} d_{p,a}}{D_a} = \frac{d_{p,a}}{L} \frac{1}{a_a} \tag{22}$$

Figures 9 and 10 show the resultant Peclet numbers plotted vs.

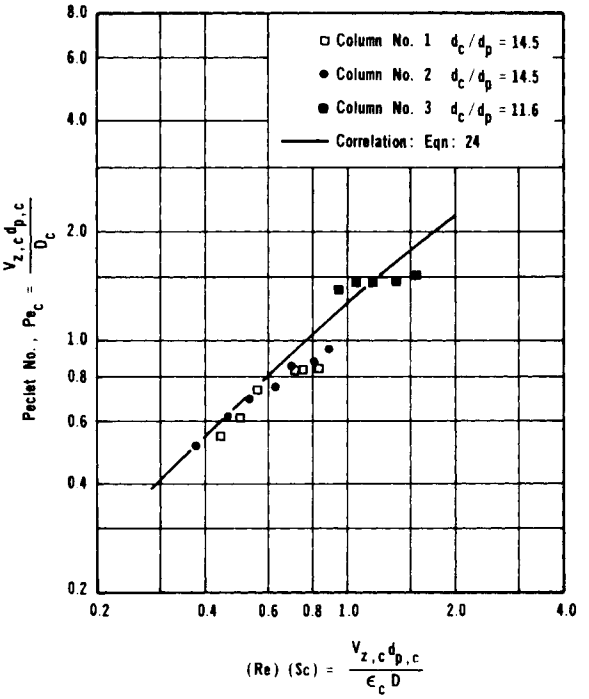

Figure 9. Axial dispersion for the core from the deconvoluted data.

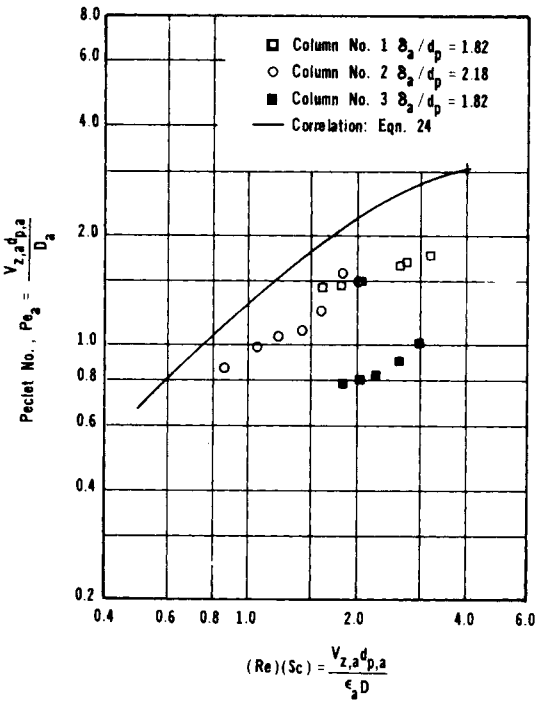

Figure 10. Axial dispersion for the annulus from the deconvoluted data.

(Re)(Sc). This product of Reynolds and Schmidt number is given, for example for the core section by

$$[(\mathrm{Re})(\mathrm{Sc})]_c = \frac{V_{zc}d_{p,c}}{\epsilon_c D} = \frac{Ld_{p,c}}{\mu_{1,o}D}\,b_c \tag{23}$$

with the analogous expression for the annulus. The line in Figure 9 for the core is a correlation (Scott et al., 1974) representing experimental data of several investigations. The data were for axial dispersion for gases in packed beds with large tube-to-particle diameter ratios; that is, for a nearly uniform porosity. The curve is represented by the equation

$$\frac{1}{(\mathrm{Pe})_c} = \frac{0.73}{[(\mathrm{Re})(\mathrm{Sc})]} + \frac{0.5}{1 + 9.7[(\mathrm{Re})(\mathrm{Sc})]^{-1}} \tag{24}$$

The curve in Figure 9 for the annulus is again a plot of Eq. 24. Our data which is for annulus-to-particle ratios, δ_a/d_p of 1.8 to 2.2, lie considerably below the correlation. This is in qualitative agreement with the results of Hsiang and Haynes (1977) who found that axial dispersion was greater in columns with a low tube-to-particle ratio (their data were for a range d_t/d_p from 1.5 to 8.2) than expected in columns with a large ratio. It is also noted in Figure 10 that Pe_a was different for columns 1 and 3, even though the particle size and δ_a in the annulus were the same. The difference in Pe_a must be due to the lack of reproducibility in packing an annulus with such a small annulus width-to-particle diameter ratio (1.8). Evidently packing under these dimensions, even with controlled packing conditions, is difficult to duplicate and the Pe vs. (Re)(Sc) relation is a characteristic of the specific bed.

PECLET NUMBERS BY CURVE FITTING THE OVERALL RESPONSE

The agreement of the Peclet numbers in Figure 9 with the correlation for large d_c/d_p suggests that Eq. 24 might be used to provide a relation between parameters a_c and b_c. Along with Eqs. 16 and 17 this permits expressing Eq. 9 for $C(1,\tau)$ in terms of but two parameters a_a,b_a. Such an approach would be useful for predicting channeling only if one section of the bed was known to have a large d_c/d_p ratio. In our experiments this was the core region, and, in general, it would be for the uniformly packed, non-channeled part of the bed.

When applicable, Eq. 24 can be combined with Eqs. 21 and 23 to relate a_c and b_c. The result is

$$a_c = \frac{d_{p,c}}{L}\left\{\frac{0.73}{b_c\dfrac{Ld_{p,c}}{\mu_{1,o}D}} + \frac{0.5}{1 + 9.7\left[b_c\dfrac{Ld_{p,c}}{\mu_{1,o}D}\right]^{-1}}\right\} \tag{25}$$

where $\mu_{1,o}$, the first moment of the overall response curve, can be evaluated directly from the experimentally measured response curve. Combining Eq. 25 with Eqs. 16 and 17 gives a_c in terms of b_a. Hence, Eq. 9 becomes a function of but two parameters, b_a and a_a. The final step is to find the values of these two parameters that, with Eq. 9, give the best agreement with the experimental, overall response curve, $C_e(1,\tau)$. The curve fitting is done by minimizing the function $F(a_a,b_a)$

$$F(a_a,b_a) = \int_o^\infty [C_{\exp}(1,\tau) - C(1,\tau,a_a,b_a)]\,d\tau \tag{26}$$

The minimization of $F(a_a,b_a)$ was accomplished by using a computer program (ZXMIN, 1981) based upon a quasi-Newton method requiring no derivatives. The method gives rapid convergence. The agreement of the experimental response curve with that predicted using the optimum values of b_a and a_a is illustrated in Figure 11, which is for column 3.

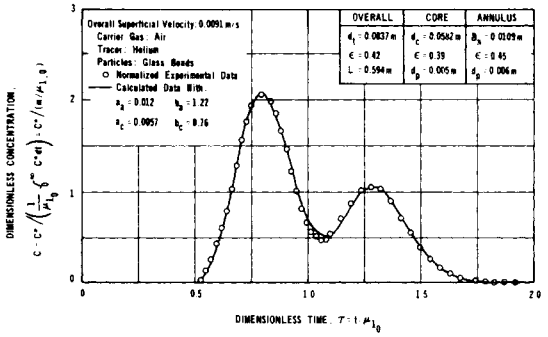

Figure 11. Experimental and calculated response curves: two-parameter fitting procedure (Column No. 3, Run #3, Noninteraction).

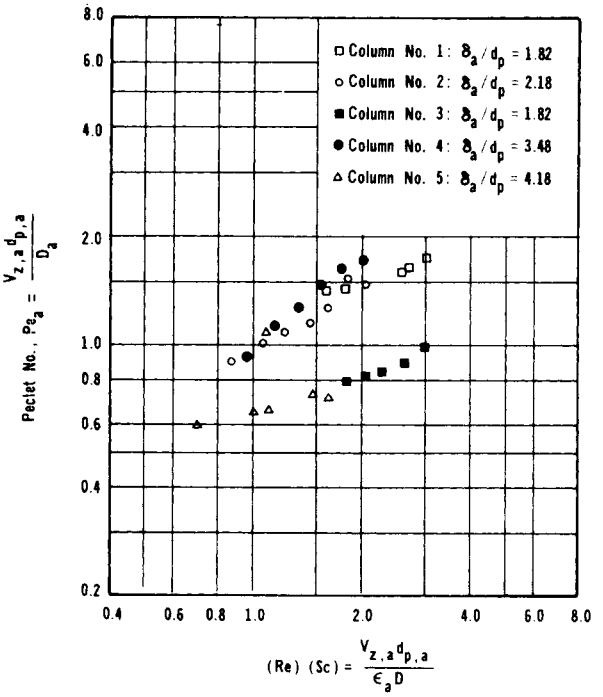

Figure 12. Axial dispersion for the annulus from two-parameter fitting procedure.

TABLE 2. PREDICTED AND EXPERIMENTAL VOID AREA

Column No.	Overall Velocity V_z, m/s	Fractional Void Area in Core, $\epsilon_c A_c/A$			Fraction of Total Flow in Core G, Predicted	
		Predicted				
		TPFP	*AM*	Exp	*TPFP*	*AM*
1	0.0093	0.20	0.21	0.21	0.27	0.28
2	0.0090	0.20	0.21	0.21	0.35	0.38
3	0.0091	0.20	0.23	0.20	0.36	0.44
4	0.0088	0.092	0.10	0.079	0.12	0.14
5	0.0094	0.25	...	0.076	0.68	...

TPFP = predicted by two-parameter fitting model (Eq. 28)
AM = predicted by approximate (t_m) model

Once a_a and b_a are evaluated, the Peclet number and (Re)(Sc) for the annulus are determined from Eq. 22 and

$$[(\text{Re})(\text{Sc})]_a = b_a \frac{L d_{p,a}}{\mu_{1,o} D} \tag{27}$$

The results for columns 1–5 are shown in Figure 12. These Peclet numbers are essentially the same as those determined by the deconvolution method for columns 1–3 and shown in Figure 10. The agreement lends confidence to the methods proposed to evaluate axial dispersion from overall response measurements. When two more-or-less distinct peaks are observed, the deconvolution method provides an attractive way to evaluate Pe for both the channel and main section. When two distinct peaks are not observed, as for columns 4 and 5, but the main section has a large d_t/d_c ratio, the second method can be used to obtain Pe for the channel section.

REPRODUCIBILITY

The random nature of packed beds means that the question of reproducibility is important. To test the effect of repacking the bed on the response curve, data were obtained for two beds at the conditions of column 5. In one sense, this column provided a severe test because channeling was mild and deviation of the response from a Gaussian curve was slight. The void fractions for this duplicate column (5R in Table 1) agreed reasonably well with values for the original bed. The response curves for beds 5 and 5R are shown in Figure 13 and the agreement is reasonable. However, it is noted that in column 5 the ratio δ_a/d_a is 4. In contrast, in columns 1 and 3, for which porosities and particle sizes in the annulus were the same, the Peclet numbers were significantly different (see Figure 10), suggesting lack of reproducibility. For the annuli in columns 1 and 3 the ratio δ_a/d_a was 1.8. These results suggest that reproducibility in repacking beds is not assured when the ratio of available distance to particle diameter is low, between 4 and 2 for our experiments.

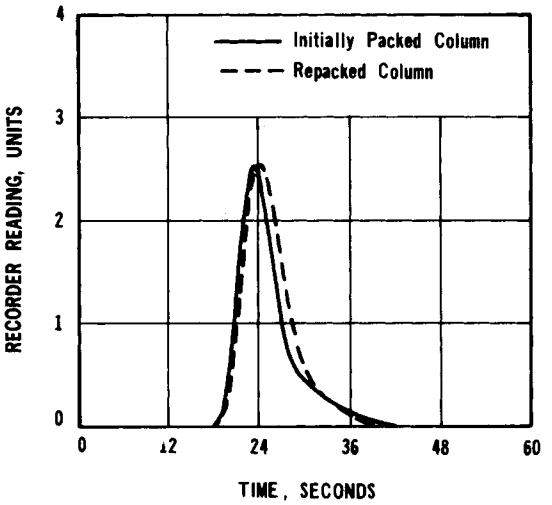

Figure 13. Reproducibility test: repacking of Column No. 5, Run No. R-2, noninteraction.

PREDICTION OF CHANNELING

Two-Parameter Model

When Peclet numbers can be calculated by the methods just described, the void areas and flow rates in the core and channel sections can be predicted. The problem is to determine the void areas $\epsilon_c A_c$, and $\epsilon_a A_a$, and $V_{z,c}A_c$ and $V_{z,a}A_a$ from the known overall void area, flow rate and overall response curve. The procedure is the reverse of the two-parameter minimization procedure described for obtaining Peclet numbers. From the known Pe_c and Pe_a, and Eqs. 16, 17, 21, and 22 two relations are obtained: one relating a_c and b_c for the core and the other relating a_a and b_a for the annulus. These relations permit expressing Eq. 9 in terms of only b_a and b_c as unknowns. This expression for predicting $C(1,\tau, b_a$ and $b_c)$ takes the form:

$$C(1,\tau,b_a,b_c) = \frac{b_a - 1}{b_a - b_c} b_c[C_c(1,\tau,b_c] + 1 - \frac{b_a - 1}{b_a - b_c} b_c[C_a(1,\tau,b_a)] \tag{28}$$

The optimal values of b_a and b_c can now be evaluated by fitting Eq. 28 to the overall response curve. The minimization technique ZXMIN may be used along with an equation analogous to Eq. 26. After b_a and b_c are determined, $\epsilon_c A_c$ and $V_{z,c}A_c$ are calculated from:

$$\epsilon_c A_c = \frac{b_a - 1}{b_a - b_c}(\epsilon A) \tag{29}$$

$$V_{z,c}A_c = G(V_z A) = \frac{b_a - 1}{b_a - b_c} b_c (V_z A) \tag{30}$$

These equations follow directly from Eqs. 14–17. Then the results for the annulus are obtained from Eqs. 16 and 17.

The suitability of this method of prediction can be determined by comparing the known void areas for the core for the five columns with $\epsilon_c A_c$ calculated from Eq. 29. The comparison is about the same for all velocities and is shown in Table 2 (TPFP vs. Exp.) for V_z of about 0.90 cm/s. The void area results are tabulated as the ratio $(\epsilon_c A_c)/A$. Also shown are the predicted fraction G of the total flow rate that is in the core. The predicted void areas agree well (<5% deviation) with the known results for columns 1–3, are about 15% in error for column 4, and greatly in error for column 5. Relating these errors to the response curves in Figures 3–7 indicates that we can predict the extent of channeling if there are two peaks in the response curve, but this is not possible when channeling causes only an elongation of the tail in the response (column 5).

This inadequacy is not due to a poor fit of Eq. 28 to the experimental response. Figure 14 for column 5 shows that the predicted response agrees well with the experimental curve. The problem is that with only a slightly asymmetric response, it is not possible to predict suitable Peclet numbers. For example, one source of error is that Eq. 24 cannot be applied to a bed where the ratio d_t/d_c is <10 as in case for column 5. A restriction of the prediction method is that suitable Peclet numbers can be ascertained only when the

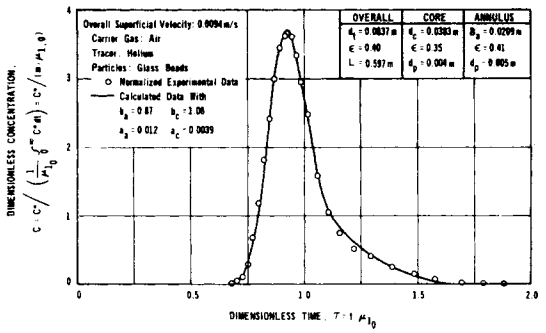

Figure 14. Experimental and calculated response curves: Column No. 5, Run #6, noninteraction.

deconvolution method, or when the uniform-bed correlation (Eq. 24, may be used.

Approximate (t_{max}) Model

Suppose that the first moments of the core and annular regions are equal to the corresponding times, $t_{m,c}$ and $t_{m,a}$, of the maximum of the concentration peaks. Now the void volumes and flow rates can be calculated without knowing Peclet numbers. Equations 14 and 15 become

$$b_c = \frac{\mu_{1,o}}{t_{m,c}} = \frac{1}{\tau_{m,c}} \tag{31}$$

$$b_a = \frac{\mu_{1,o}}{t_{m,a}} = \frac{1}{\tau_{m,a}} \tag{32}$$

Substituting these values for b_c and b_a into Eqs. 29 and 30 give the following simple expressions for void area and fraction of the flow in the core:

$$\frac{\epsilon_c A_c}{A} = \frac{\dfrac{1}{\tau_{m,a}} - 1}{\dfrac{1}{\tau_{m,a}} - \dfrac{1}{\tau_{m,c}}} \tag{33}$$

$$G = \frac{\dfrac{1}{\tau_{m,a}} - 1}{\dfrac{1}{\tau_{m,a}} - \dfrac{1}{\tau_{m,c}}} \left(\frac{1}{\tau_{m,c}}\right) \tag{34}$$

These results are equivalent to the solution of Eqs. 14–17 for the four unknowns: $\epsilon_c A_c$, $\epsilon_a A_a$, $V_{z,c}$, $V_{z,a}$. For columns 1–4 it is possible to estimate values of $t_{m,c}$ and $t_{m,a}$. Table 2 gives the results for $\epsilon_c A_c/A$ and G calculated from Eqs. 33 and 34 for these columns. For columns 1 and 2 the agreement with the known values of $\epsilon_c A_c/A$ is good, while for columns 3 and 4 the deviation is 15 and 27% respectively. For column 5 the method cannot be applied because $t_{m,a}$ cannot be estimated from the response curve (Figure 7).

It is concluded that this approximate method is nearly as satisfactory as the more complicated methods when the section of the response curve is not influenced by the other section as in Figures 3 and 4. It is only for column 4 (Figure 6) that the more complex method requiring Peclet numbers gives significantly better results. Note that in column 4 the response peak for the core was not distinct. This qualitative conclusion can be made quantitative by developing equations for the fractional difference between $t_{m,c}$ and the first moment $\mu_{1,c}$ for the core and also between $t_{m,a}$ and $\mu_{1,a}$. This is done by solving Eqs. 1 and 2 for $C_c(1,\tau)$ and $C_a(1,\tau)$ with the boundary conditions for a long bed for which $C_c = C_a = 0$ for $z \to \infty$. The final form of the equations gives a complex expression for the fractional differences in terms of a_c and a_a (or the Peclet numbers). The final equations and their derivation are available (Oliveros, 1981).

ANALYSIS OF MULTIPLE-PEAK RESPONSE CURVES

In packed beds with diameters of the order of bed depth, multiple channels may exist. Evidence for this are the multiple-peak response curves that have been observed in tracer tests of *in-situ*, oil-shale retorts. In general, two parameters a_i and b_i are necessary to define the i-th channel. For multiple channels the number of parameters to be evaluated from the response curve becomes too large for useful results. However, if multiple peaks are observed and these peaks can be deconvoluted, approximate values for $\epsilon_i A_i$ and G_i can be obtained. Equating the tracer entering the i-th channel to that leaving the same channel gives

$$Q_i M = Q \int_i C^* \, dt \tag{35}$$

where M is the strength of the pulse. The strength of the pulse is given by the area under the complete response curve:

$$M = \int_o^\infty C^* \, dt \tag{36}$$

Combining Eqs. 35 and 36 shows that the fraction G_i of the flow in channel i is equal to the area of the response peak for channel i divided by the area under the complete response:

$$G_i = \frac{Q_i}{Q} = \frac{\int_i C^* \, dt}{\int_o^\infty C^* dt} \tag{37}$$

The time, $t_{m,i}$, corresponding to the maximum concentration of the i-th peak can be read from the response curve. Then the void area of the channel, $A_i \epsilon_i$ is calculated from the equation

$$t_{m,i} = \frac{L(A_i \epsilon_i)}{Q_i} \tag{38}$$

Equations 37 and 38 provide a simple, but approximate method for estimating the flow rate and void area of each channel from the combined response curve, provided that the area and $t_{m,i}$ of the response peak for each channel can be identified. The method requires, in addition, that each channel be separated from every other channel. Otherwise, Eq. 37 is not valid.

ACKNOWLEDGMENT

The financial support of National Science Foundation Grant CPE-8025831 and a fellowship from FONINVES of Venezuela are gratefully acknowledged.

NOTATION

A = total cross-sectional area of the column, m^2; A_a and A_c are void plus nonvoid areas of the annulus, and core

a_a = reciprocal Peclet number for the annulus, based upon column length, $D_{z,a}/LV_{z,a}$

a_c = reciprocal Peclet number for the core region, based upon column length, $D_{z,a}/LV_{z,c}$

b_a = relative interstitial velocity in the annulus, $\epsilon V_{z,a}/\epsilon_a V_z$

b_c = relative interstitial velocity in the core, $\epsilon V_{z,c}/\epsilon_c V_z$

C^* = concentration kg-mol/m^3

C_a, C_c = dimensionless concentrations in the annulus and core, $C_a^*/C_o^*, C_c^*/C_o^*$; C_o^* = concentration in the pulse
$= MV_z/\epsilon L$
$= (1/\mu_{1,o}) \int_o^\infty C^* \, dt$

$C_{c,d}$ = conc. in deconvoluted response for the core section

C_{exp} = experimentally measured concentration, kg·mol/m^3

$D_{z,a}D_{z,c}$ = axial dispersion coefficients in the annulus and core, respectively

D = diffusivity of the flowing gas, m^2/s

d_t = diameter of the column: d_c = diameter of the core, m

$d_{p,a},d_{p,c}$ = diameters of the glass beads in the annulus and core, m

F = function to be minimized, Eqs. 20 and 26

G = fractional flow rate, Q_c/Q, in the core

L = length of packed column, m

M = strength of pulse input, $\int_o^\infty C^* \, dt$, kg·mol/m^3

Pe_a = Peclet number in the annulus, $V_{z,a}d_{p,a}/D_{z,a}$

Pe_c = Peclet number in the core, $V_{z,c}d_{p,c}/D_{z,c}$

Q_a = volumetric flow rate in annulus, m^3/s; Q_c refers to core and Q represents total flow rate

$[(Re)(Sc)]_a$ = Reynolds number times Schmidt number for the annulus, $V_{z,a}d_{p,a}D/\epsilon_a$

t = time, s; t_m = time corresponding to the maximum concentration in the response curve

V_z = overall superficial velocity, m/s; $V_{z,a}$ and $V_{z,c}$ are superficial velocities in the annulus and core

Z = dimensionless length of packed bed, z/L

z = axial dimension in packed column, m

Greek Letters

δ_a = width of the annulus, m

$\delta(\tau)$ = Dirac-delta function, s^{-1}

ϵ = overall void fraction for the entire column; ϵ_a and ϵ_c are void fractions in the annulus and core regions

μ_1 = first moment of response curve, s; $\mu_{1,o} = \epsilon L/V_z$, refers to the overall response curve; and $\mu_{1,a}$ and $\mu_{1,c}$ to the annulus and core regions as defined by Eqs. 12 and 13

τ = dimensionless time, $t/\mu_{1,o}$ or $tV_z/\epsilon L$

$\tau_{m,a}$ = dimensionless time corresponding to the maximum concentration in the response curve for the annulus, $t_{m,a}/\mu_{1,o}$; $\tau_{m,c} = t_{m,c}/\mu_{1,o}$

σ = variance of the response curve, s

Subscripts

c = core section

a = annulus

i = channel i

LITERATURE CITED

Danckwerts, P. V., "Continuous Flow Systems; Distribution of Residence Times," *Chem. Eng. Sci.*, **2**, 1 (1953).

Ergun, S., "Fluid Flow through Packed Columns," *Chem. Eng. Prog.*, **48**, 89 (1952).

Hsiang, C. T., and H. W. Haynes, Jr, "Axial Dispersion in Small Beds of Large Spherical Particles," *Chem. Eng. Sci.*, **32**, 678 (1977).

Oliveros, G., "Dynamic Experiments for Studying Channeling in Packed Beds," Ph.D. Thesis, Univ. of California, Davis (1981).

Schwartz, C. E., and J. M. Smith, "Flow Distribution in Packed Beds," *Ind. and Eng. Chem.*, **45**, 1209 (1953).

Stanek, V., and V. Eckert, "A Study of Area Porosity Profiles in a Bed of Equal-Diameter Spheres," *Chem. Eng. Sci.*, **34**, 933 (1979).

Wen, C. Y., and Fan, L. T., "Models for Flow Systems and Chemical Reactors," Marcel Dekker Inc., New York (1975).

Wehner, J. F., and Wilhelm, R. H., "Boundary Conditions of Flow Reactor," *Chem. Eng. Sci.*, **6**, 89 (1956).

ZXMIN, "A Computer Program for Minimizing a Function of N Variables," University of California, Davis, Computer Center (1981).

Manuscript received July 10, 1981; revision received October 29, and accepted November 5, 1981.

Heat Transfer to Horizontal Tubes in the Freeboard Region of a Gas Fluidized Bed

Overall heat transfer coefficients were measured for an instrumented horizontal tube of diameter 25 mm in the feedboard region above fluidized beds of 102 μm, 470 μm and 890 μm sand in a 0.25 m × 0.43 m × 3.0 m tall pilot scale column. The superficial air velocity varied from near minimum fluidization to 1.7 m/s. The instrumented tube was placed at different positions in a 16-tube bundle. The measured heat transfer coefficients were bounded for tubes near the expanded bed surface by the immersed tube values, and for remote tubes by the values for particle-free air in crossflow. The results are correlated within ±12% by a simple equation which incorporates these limits. The results are in good qualitative and quantitative agreement with previous experimental results.

S. E. GEORGE and J. R. GRACE

Department of Chemical Engineering and Coal Research Centre University of British Columbia Vancouver, Canada V6T 1W5

SCOPE

The freeboard region above gas fluidized beds may contain heat transfer tubes for a number of different reasons, e.g., for waste heat recovery, quenching of reaction products, or because of variation in bed level, as in fluid bed combustors during turndown. The tubes are most often horizontal and unfinned. While there have been many studies of heat transfer to tubes immersed inside fluidized beds, tubes in the freeboard region have received scant attention. Experimental results and design methods are required which will allow heat transfer rates to be estimated for tubes in the freeboard region.

In the present study, heat transfer measurements for horizontal unfinned tubes have been carried out in a pilot scale column. Variables have included particle size, superficial air velocity, static bed depth, position within the tube bundle and horizontal pitch. Comparison is given with previous work and with heat transfer for immersed tubes and with tubes subject to crossflow of particle-free air.

S. E. George is presently with the Shell Canada Research Center, Oakville, Canada L6J 5C7.

The experimental work described in this paper was carried out at McGill University, Montreal, Canada.

0001-1541-82-3116-0759-$2.00.